

# Effects of low-energy impact at different temperatures on residual properties of adhesively bonded single-lap joints with composites substrates

Wei Huang<sup>a,b,c</sup>, Lingyu Sun<sup>a,b,c,\*</sup>, Yang Liu<sup>a,b,c</sup>, Yantao Chu<sup>a,b,c</sup>, Jinxi Wang<sup>a,b,c</sup>

<sup>a</sup> *School of Transportation Science and Engineering, Beihang University, Beijing, 100191, China*

<sup>b</sup> *Lightweight Vehicle Innovation Center, Beihang University, 37 Xueyuan Road, Haidian District, Beijing 100191, China*

<sup>c</sup> *Beijing Hangshu Vehicle Data Institute Co., Ltd, Beijing 100062, China*

\* Corresponding author. *E-Mail address:* lysun@buaa.edu.cn (Lingyu Sun).

## Abstract

This paper evaluates the influence of temperature, stiffness combination and impact energy on residual tensile properties of adhesive single-lap joints (SLJs) with composite substrates. High-strength steel (HSS), glass and carbon fiber reinforced plastics (GFRP and CFRP) were chosen as adherends, while Araldite® 2015 was the adhesive. The effects of four temperatures (-40, 23, 50 and 80 °C) were taken into account for the transverse impact loading with three different energy levels of 0.5, 1.5 and 2.5 J. Residual behavior and failure modes were investigated through secondary tensile tests at ambient temperature. The results indicated that impact energy and temperature both have a strong correlation with residual static properties. The degradation of mechanical strength, induced by the combined effect of low-energy impact loading and temperature, was particularly pertinent for the joints with dissimilar substrates. Furthermore, increasing the relative stiffness ratio can enhance the residual tensile strength of the SLJs with composites.

**Keywords:** Adhesive joints; Low-energy impact; Temperature influence; Residual strength; Damage of structures.

## 1. Introduction

Continuous fiber/epoxy laminated composites are used extensively by the aerospace and automotive industries due to their light weight and excellent formability [1-3]. It is well known that conventional connecting methods, such as fasteners, are highly likely to cause fiber cutting and matrix damage, thereby introducing stress and destroying structural integrity. Unlike traditional methods, however, adhesive bonding is capable of connecting different materials without degrading the mechanical properties of the substrates, and it also presents advantages of design flexibility and easy fabrication [4]. However, these structures are inevitably exposed to low-energy impact (energies below 3.7 J [5,6]) incidents during manufacture, operation and transportation, as well as during maintenance. Low-energy impact loads such as falling tools, hail and debris could sacrifice the safety performance to a certain extent [7,8]. Moreover, these types of structure are known to operate at variable temperatures in different regions of the world [9], so the bonded structures may have different sensitivities to low-energy impact load at different ambient temperatures. Under the synergistic effect of temperature and impact load, different degrees of degradation exist, such as non-visual effects or barely visible impact damage (BVID). This initial damage encountered in SLJs can lead to in-service damage propagation, causing degradation of the composite structure [10-13]. Therefore, an investigation of the residual properties of SLJs after impact and temperature treatment is necessary to avoid catastrophic failure during operation.

Hitherto, the residual properties of composite bonded joints after the simultaneous effect of transverse impact loads and temperature have not been studied, but many researchers have studied the impact failure behavior. Vaidya et al. [14] reported the effects of transverse impact loading on the mechanical properties of SLJs where they found a higher concentration of peel stress in their structures but, in contrast, in-plane impact tests produced less peel stress concentration. Another study concerning transverse impacts was conducted by Kim et al. [15] where numerical simulations and experiments were performed on glass-epoxy bonded joints to identify their damage modes induced by transverse impacts. The main conclusion derived from this work was that localized debonding around the impact point arose from the transverse shear stress

generated within the adhesive structure. Sankar et al. [16] reported the dynamic properties of bonded joints containing two different types of adherend, where the impact strength of butt joints using two types of metal, aluminum and steel, was assessed as a function of the substrate stiffness. They concluded that, for joints with different types of substrate, the joint strength in tension appears to be lower than for joints made of similar materials. Likewise, Huang et al. [17] carried out experiments and simulations of transverse impact and fatigue on SLJs containing various combinations of composite and metal panels. They found that the combination of adherends dramatically affects the fatigue life of the entire structure, with the highest strength occurring in samples made with the same substrate. Oztoprak et al. [18] evaluated the degradation of mechanical properties of aluminum/glass fiber composite SLJs after impact. After applying an impact load of 2.5 J to specimens, it was found that their failure strength exhibited a significant reduction. Not only can the low-energy impact load change the characteristics of the bonded structure, but the temperature also causes a change in the toughness and thermal expansion coefficient of the adhesive and adherends, and subsequently leads to premature failure [19].

Grant et al. [20] investigated the behavior of SLJs and T joints at -40 °C and 90 °C experimentally and analytically. According to their results, a reduction in the adherend yield stress, together with the failure envelope, results from the increase in temperature. Sayman et al. [21] experimentally examined the influence of temperature on the performance of composite bonded joints. Different impact energy levels were imposed at room temperature. Then, tensile tests at -20 °C, 23 °C, 50 °C and 80 °C were applied to assess the joint durability. They found that extreme test temperatures seemed to weaken the static load-capacity of joints. Also, load carrying capacity decreased when the specimens were subjected to 5, 10 and 15 J impact loadings; while their load capacity showed an abnormal improvement after 20 J impact resulting from the perforation damage producing higher strength. Previous works by Sayman et al. [22] employed axial tensile impact tests under different temperature environments to determine the residual mechanical strength of composite SLJs. They showed that, under higher energy impact loading or more severe temperature environments, the joint

strength became weaker than its normal level. More recently, the works performed by Avendaño et al. [23] indicated that the behavior of SLJs under static tensile and impact loadings altered with temperature in the range from -30 °C to 80 °C. The increase in temperature aggravates the influence of the strain rate on the failure response of SLJs to a certain extent, and higher joint failure strength can be found at high strain rates compared to lower strain rates.

Hitherto, nearly all studies solely report impact or temperature response of adhesively bonded joints, rather than their residual properties after being subjected to low-energy impact at different temperatures. Also, the existing studies on joints under the combined effects of impact and temperature have mostly focused on metallic materials or joints with similar substrates, and the effect of material combinations on residual structural performance was not quantitatively characterized. Thus, this paper seeks to determine the residual strength of bonded joints after impact tests at different impact levels and various temperatures, which, for the first time, could forecast the links between impact energy, temperature and stiffness combination of the joints, along with the synergy between these factors. The low-energy transverse impact tests with three energy levels were carried out under four distinct environments prior to axial tensile tests at normal temperature conditions.

## **2. Materials**

### *2.1. Properties of materials*

The composite SLJs were made up of carbon and glass composite laminates, high strength steel and a polymeric adhesive with excellent bonding properties. The composite panels with layers of  $[0^\circ/90^\circ]_{4s}$  were made from GFRP and CFRP prepregs and epoxy resin fabricated by Shandong Dingsheng Co., Ltd. The CFRP panels were comprised of Toray® T700SC-12000-50C carbon fiber and KH1301 epoxy resin, with a resin content of  $36\pm 2$  vol%. The glass fiber laminates contained E-glass fiber and KH1301 epoxy resin with resin content of  $34\pm 2$  vol%. The corresponding mechanical properties of each ply are listed in Table 1, where  $E_1$ ,  $E_2$  and  $E_3$  stand for Young's modulus in different directions.  $G$  and  $\mu$  represent their shear modulus and Poisson's

ratio, respectively. Here, high strength steel DP 590 used as structural material in the automotive industry was selected as the metal material for the SLJs. These plates with specified dimensions were bonded by epoxy adhesive Araldite® 2015, a two-component structural adhesive that has been adopted in a considerable body of literature [24-26]. Its material properties are given in Table 2.

**Table 1** Mechanical properties for the composite adherends.

Mechanical properties	CFRP	GFRP
$E_1$ (GPa)	128.0	30.50
$E_2$ (GPa)	8.7	6.90
$E_3$ (GPa)	8.7	6.90
$\mu_{12}$	0.32	0.34
$\mu_{13}$	0.32	0.34
$\mu_{23}$	0.30	0.46
$G_{12}$ (GPa)	4.0	4.65
$G_{13}$ (GPa)	4.0	4.65
$G_{23}$ (GPa)	2.4	1.60

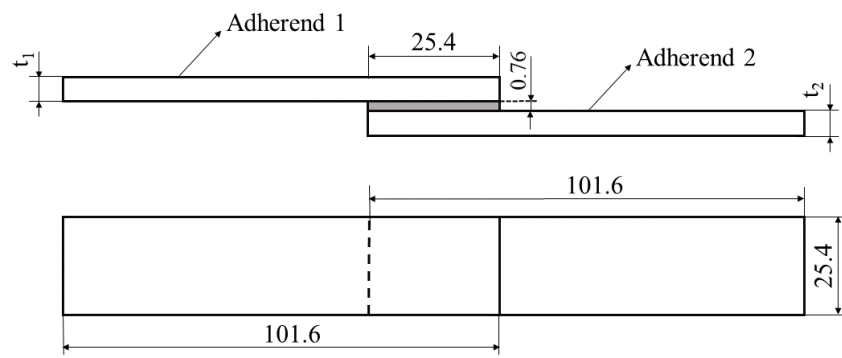
**Table 2** Material properties for Araldite® 2015 [24].

Araldite® 2015	
Young's modulus, $E$	1.83 GPa
Glass transition temperature, $T_g$	65±5 °C
Poisson's ratio, $\mu$	0.33
Tensile strength, $\sigma$	21.63 MPa
Shear modulus, $G$	0.56 GPa
Shear strength, $\tau$	17.9 MPa

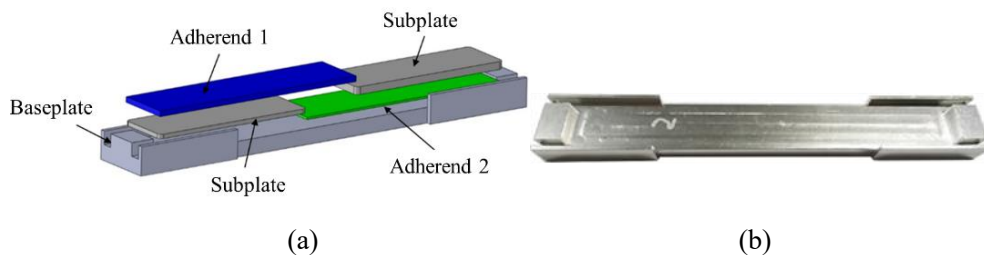
## 2.2. Preparation of specimens

Four types of composite specimen were adopted, viz. CFRP/CFRP, CFRP/HSS, GFRP/GFRP and GFRP/HSS assembled SLJs. Their geometry and dimensions are shown schematically in Fig. 1, which were in accordance with ASTM D5868 [27]. The

thickness of laminated composite and metal panels were 2.5 and 2 mm, respectively. A 0.76 mm adhesive thickness was controlled by a stainless-steel mold, as shown in Fig. 2(a) and (b). The baseplate and two different thickness metal subplates were applied to control total length and lap length of joints, respectively. Also, in order to ensure the bond quality, the bonding area of both adherends was roughened by sandpaper and then cleaned using 75% alcohol. The preformed SLJs specimens, with assembled molds, were then cured at room temperature for more than 20 h. The completed adhesion samples are shown in Table 3.


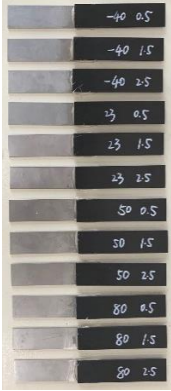




**Fig. 1.** Schematic diagram of the SLJ specimen.



**Fig. 2.** Schematic diagram of the mold for fabrication of the SLJs: (a) assembling the joints; (b) removing specimens [28].

**Table 3** Four types of SLJ samples.

No.	#1	#2	#3	#4
Adherend 1	CFRP (2.5 mm)	CFRP (2.5 mm)	GFRP (2.5 mm)	GFRP (2.5 mm)
Adherend 2	CFRP (2.5 mm)	HSS (2 mm)	GFRP (2.5 mm)	HSS (2 mm)
Sample				

### 3. Experimental procedure

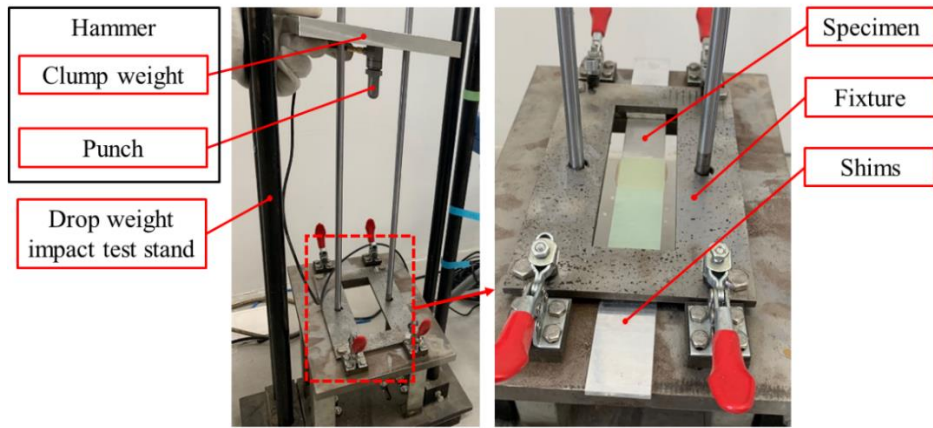
This section presents the process of drop-weight impact and static tensile testing. First, impact experiments were conducted on the four types of composite specimen at different temperatures to assess how different parameters may influence the structural integrity of joints. Then, tensile tests were employed to measure the residual tensile mechanical properties. All conditions for the experiments are given in [Table 4](#).

**Table 4** All the working conditions for four types of adhesively bonded SLJs.

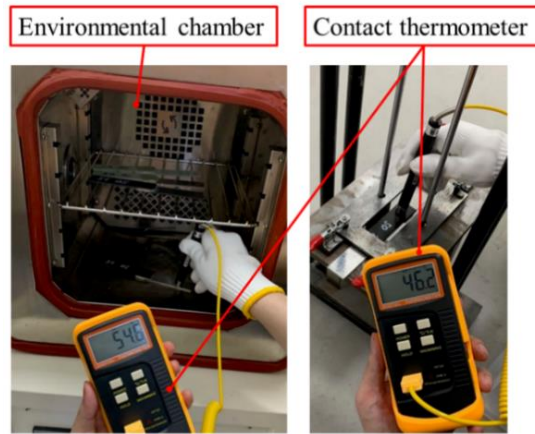
Temperature $T$ (°C)	Impact energy $E$ (J)		
	0.5	1.5	2.5
-40	#1, #2, #3, #4	#1, #2, #3, #4	#1, #2, #3, #4
23	#1, #2, #3, #4	#1, #2, #3, #4	#1, #2, #3, #4
50	#1, #2, #3, #4	#1, #2, #3, #4	#1, #2, #3, #4
80	#1, #2, #3, #4	#1, #2, #3, #4	#1, #2, #3, #4

#### 3.1. Low-energy impact tests

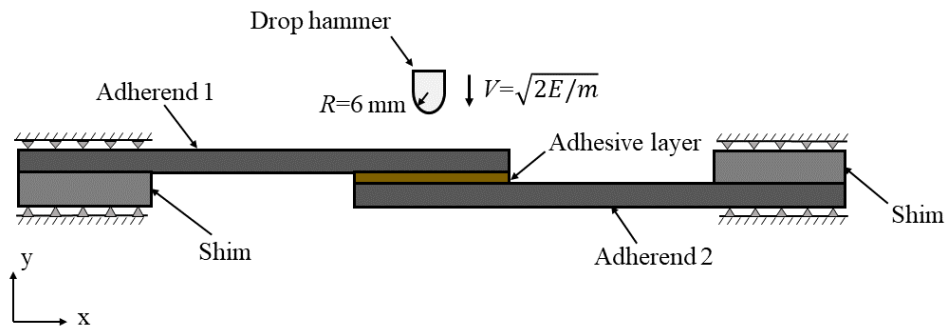
A self-designed impact system was employed for the drop weight impact tests, see [Fig. 3](#), and an environmental chamber with digital temperature control between -60 °C and 100 °C was used, as shown in [Fig. 4](#).



**Fig. 3.** Impact setup for low-energy impact tests.



**Fig. 4.** The environmental chamber and temperature measurement.



**Fig. 5.** Schematic diagram of the SLJs loaded in the low-energy impact tests by a drop hammer.

Impact tests employed three different impact energy levels  $E$  of 0.5, 1.5 and 2.5 J. Fig. 5 shows the schematic diagram of the samples loaded by a drop hammer. Each adhesive specimen was fixed with shims using the customized fixture during the tests.



The total impactor mass  $m$  was 665 g; and, it could impact with velocity  $v$  ranging from 1.23 to 2.74 m/s, which is calculated from:

$$v = \sqrt{2E/m} \quad (1)$$

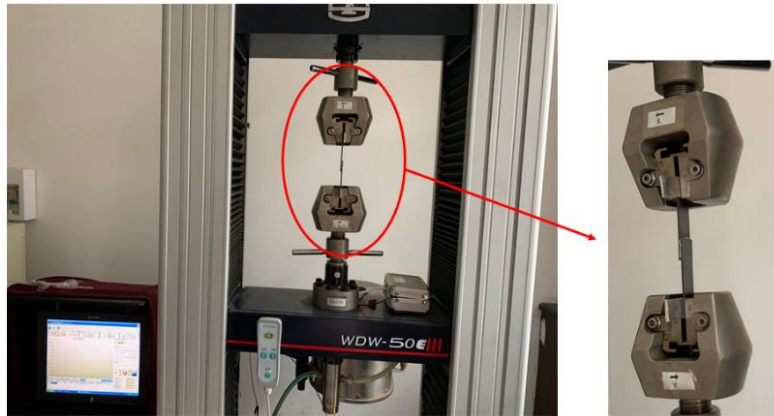
The impact hammer was dropped from a series of heights  $h$  that ranged from 77 to 384 mm to yield the impact kinetic energy  $E$ , which is expressed as follows:

$$h = E/mg \quad (2)$$

Since the temperature environment chamber cannot be installed on the self-designed drop weight test equipment, it was necessary to operate the chamber near the impact test machine. The samples were kept in the temperature chamber set at 55 °C until a uniform temperature was reached, they were then quickly fastened to the impact machine with the aim of bringing their temperature to the required 50 °C during the impact test. The temperature of each specimen was measured by a contact thermometer, HY 101, with an accuracy of 0.1 °C. After the impact test was executed, the external surface temperature of the sample was not lower than 46 °C, as shown in Fig. 4. Likewise, other temperature conditions, such as -40 and 80 °C, were achieved with a similar procedure.

### 3.2. Secondary tensile tests

To reveal how two important parameters, impact energy  $E$  and temperature  $T$ , influence the residual mechanical properties of the bonded joints, unidirectional tensile tests were carried out on a universal testing machine with a capacity of 100 kN, as shown in Fig. 6. In addition, alignment sheets were embedded in the grips of the test machine to reduce the bending moment stemming from the SLJs. Tensile force versus displacement curves were obtained from the tensile testing system computer.

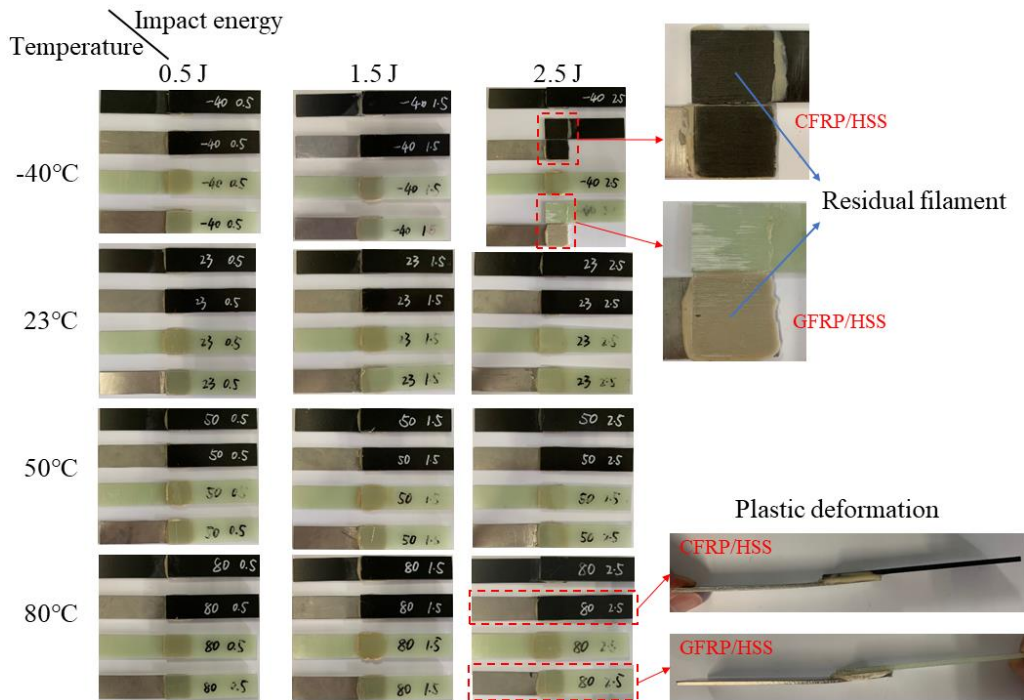


**Fig. 6.** Quasi-static tensile test set-up.

## **4. Results**

### *4.1. Low-energy impact tests*

[Fig. 7](#) shows the damage morphology for twelve different operating conditions. It is worth highlighting that there were no obvious dents appearing on the external surface of all the samples. Nevertheless, in the case of 2.5 J impact tests at  $-40\text{ }^{\circ}\text{C}$ , CFRP/HSS and GFRP/HSS specimens both failed during the impact tests. The main failure mode for these types of joint is fiber tearing with carbon or glass fibers appearing on the fracture surface. The results indicated that the adherend may be more sensitive to low temperature compared to the adhesive. Thus, the bending load of the transverse impact causes delamination failure of the adherend, especially a mismatched stiffness joint is more sensitive to such a load; In the case of 2.5 J impact tests at  $80\text{ }^{\circ}\text{C}$ , the joints with metal adherend softened, absorbing a large amount of impact energy to cause plastic deformation.

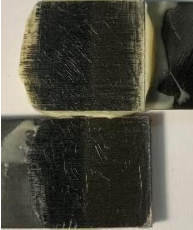



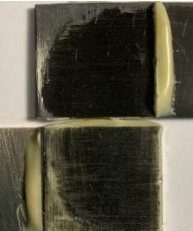

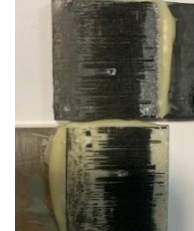


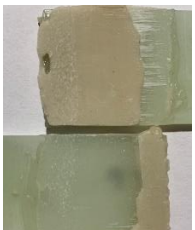


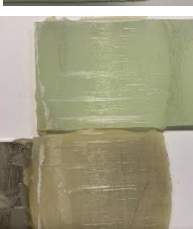





**Fig. 7.** Damage morphologies of composite joints resulting from the impact tests performed under twelve different conditions.

#### 4.2. Quasi-static tensile tests and damage mechanism

Table 5 summarizes the different fracture surfaces of bonded structures under uniaxial tension. Note that, for the case of the lower temperature conditions, the fracture surface exhibited delamination of the composite panels. However, for the medium temperature and high temperature conditions, the tensile failure mode was cohesive failure, with adhesive remaining on the fracture surfaces, as seen in Table 5. This reflected that the failure sites will depend on the environmental temperature. Because the impact loading at different temperatures may lead to initial damage at different locations, such as fiber local fracture or adhesive microcracks, this was followed by tensile tests that cause the delamination or adhesive damage to extend until bonded structural failure occurs. Moreover, it is possible to observe from the figure that dispersion of residual adhesive on the fracture surface of joints with dissimilar adherends was relatively uneven.

**Table 5** Representative fracture surfaces of four types of SLJ caused by the tensile tests after impact at different temperatures.

Adherend combination	-40 °C	23 °C	50 °C	80 °C
#1				
#2				
#3				
#4				

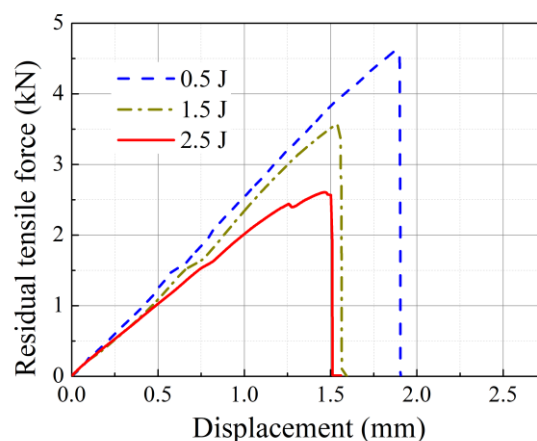
The typical load-displacement curves for CFRP/CFRP SLJs resulting from tensile testing are given in Figs. 8-14. It can be seen from Fig. 8 that the specimen for 0.5 J energy condition exhibited higher tensile peak load and displacement compared to other impact energies. As impact energy increased, both tensile peak load and displacement gradually declined. The slopes of linear segments were taken as the structural stiffness of the SLJs, which declined with increased impact kinetic energy up to 2.5 J. It can be inferred that there was obvious mechanical degradation of bonded joints under higher impact energy at -40 °C.

Relatively regular tensile failure characteristics occur after impact at room

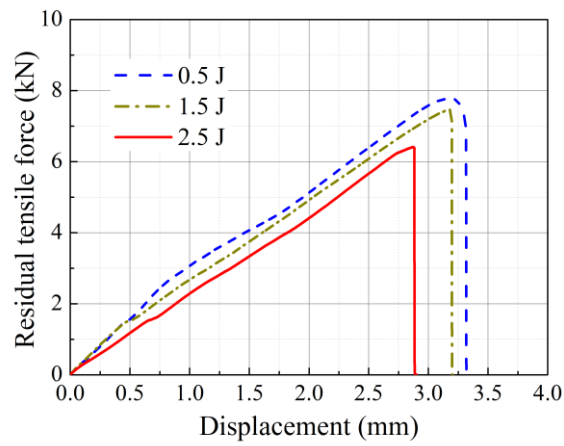
temperature, which is evident from Fig. 9. There are gradual reductions in the structural stiffness, tensile force and displacement of SLJs at room temperature. In other words, the failures of the subsequent tensile tests may be predicted from the energy level of impact at room temperature. Compared with room temperature, the joint exhibited brittleness at -40 °C, the failure strain and tensile strength decreased by 47.8% and 58.3%, respectively (2.5 J).

It is interesting to note that the impact tests at 50 °C produced different tensile failure behavior of SLJs, as recorded in Fig. 10. With the increase of impact energy, adhesive joints exhibit relatively better residual load-bearing capability. The reason is that, as the temperature rises to near the  $T_g$  zone, the adhesive material is more susceptible to deformation, so the cohesive strength exceeds the elastic modulus of the adhesive, hence impact implemented at specific temperatures seems to have some sort of crack blunting effect on the adhesive materials, making the crack tip inside the adhesive deformed and blunt [29-32].

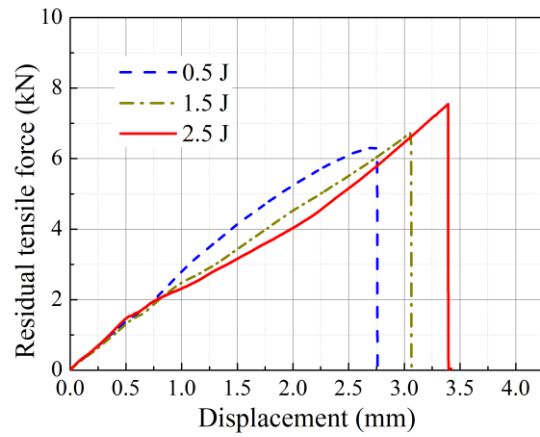
Similar to the results after impact at low temperature, the failure displacements, loads and slopes of the load-displacement curves also dropped at 80 °C as impact energy increased (see Fig. 11). However, the same crack blunting effect did not appear for 80 °C tests. It is possible that, at this temperature, the crack blunting mechanism is insufficient to compensate for the attenuation of adhesive properties due to high temperature, leading to a decline in residual performance of SLJs.



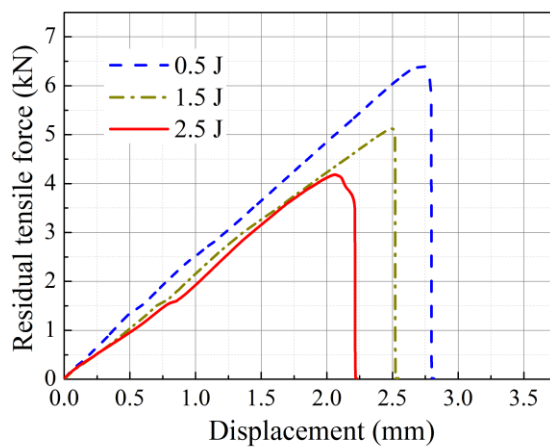
**Fig. 8.** Residual tensile load-displacement curves ( $T = -40$  °C, CFRP/CFRP).



**Fig. 9.** Residual tensile load-displacement curves ( $T = 23\text{ }^{\circ}\text{C}$ , CFRP/CFRP).



**Fig. 10.** Residual tensile load-displacement curves ( $T = 50\text{ }^{\circ}\text{C}$ , CFRP/CFRP).

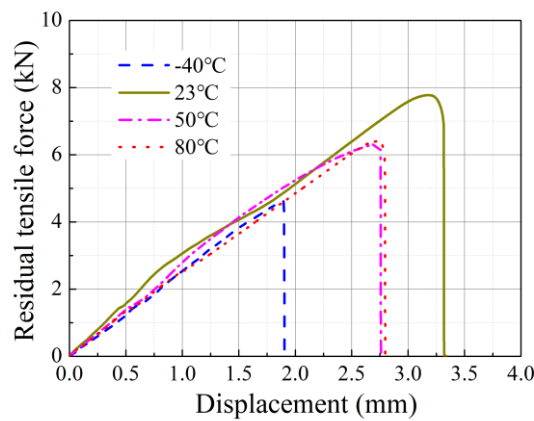


**Fig. 11.** Residual tensile load-displacement curves ( $T = 80\text{ }^{\circ}\text{C}$ , CFRP/CFRP).

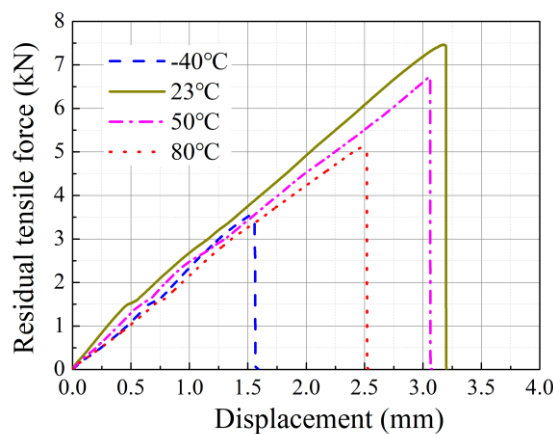
The curves shown in Fig. 12 reveal that temperatures other than room temperature have a negative impact on the residual load-bearing capability of the SLJs, and it

appears to be more significant at low temperature compared to high temperature. In addition, the maximum residual energy absorption can be seen in the curve for 23 °C, while the minimum absorption seems to be at the condition of -40 °C. Just like Fig. 12, the joints impacted at a higher energy level have similar residual characteristics, as shown in Fig. 13.

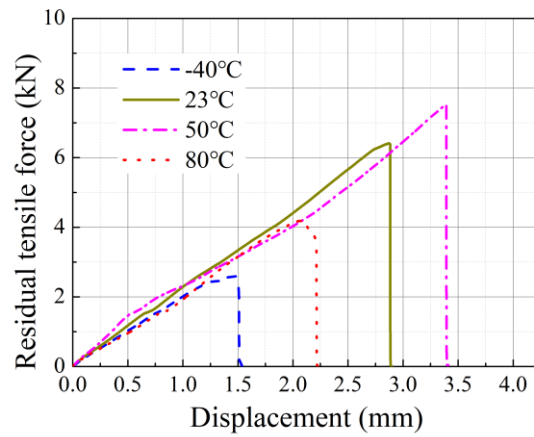
The 2.5 J impacts performed at 50 °C appear to have an enhancing effect on failure load and displacement in tensile tests, as shown in Fig. 14. The joints under this condition were found to have much higher residual strength and failure strain than the joints tested at other temperatures.



**Fig. 12.** Residual tensile load-displacement curves ( $E = 0.5$  J, CFRP/CFRP).



**Fig. 13.** Residual tensile load-displacement curves ( $E = 1.5$  J, CFRP/CFRP).

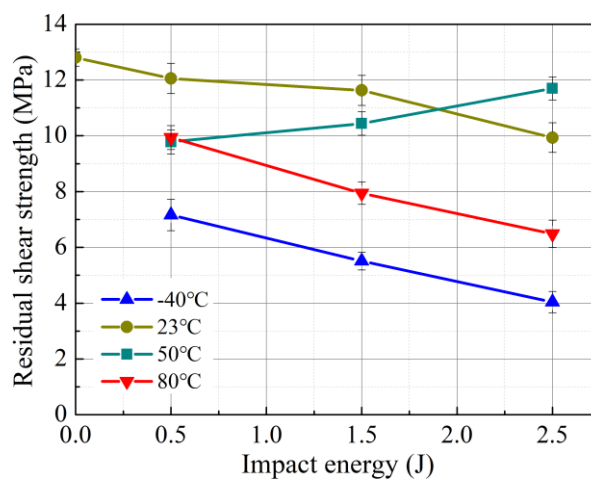


**Fig. 14.** Residual tensile load-displacement curves ( $E = 2.5$  J, CFRP/CFRP).

## 5. Discussion

### 5.1. Effects of impact energy $E$

Fig. 15 shows plots of the variation of the residual strength in tension of CFRP/CFRP specimens as a function of impact kinetic energy  $E$ . There is a strong connection between impact energy and post-impact properties of SLJs. Under impact loading at 50 °C, the residual bond strength increased with the impact energy level due to some crack blunting in the adhesive layer, while the strength dropped at other temperature conditions.

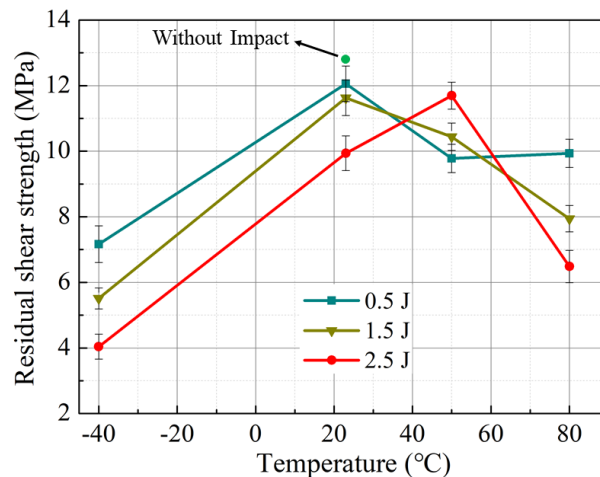


**Fig. 15.** Residual tensile strength after impact at various temperatures as a function of impact energy (CFRP/CFRP).



### 5.2. Effects of temperature $T$

Fig. 16 confirms that temperatures other than room temperature have a strong influence on the residual properties of the SLJs. It is also clear that the joints tested at extreme temperature conditions ( $-40$  or  $80$  °C) show more variation of the residual strength than those tested at  $23$  °C. Thus, the effect of impact energy on residual tensile properties increases as the absolute temperature difference (the temperature during impact tests minus room temperature). Furthermore, under  $0.5$  J impact load conditions, the residual joint strength after impact at  $80$  °C was slightly improved compared with the  $50$  °C condition. It is possible that, at particular combinations of temperature and impact energy, the residual joint strength could reach the level of non-impact conditions.



**Fig. 16.** Relationship between residual tensile strength, temperature and impact energy (CFRP/CFRP).

### 5.3. Effects of adherend combination

A comparison of the tensile failure strength of the four types of composite SLJs after  $1.5$  J impact at different temperatures is shown in Fig. 17. It can be seen that the effect of temperature varied with different types of adhesive joint, and the GFRP/GFRP joints exhibit the largest residual strength, while the residual strength of CFRP/HSS joints is the lowest. The principal cause behind this may be that the GFRP laminate is less rigid than the CFRP laminate, so the GFRP laminate absorbs more energy under the same conditions, allowing the adhesive layer to absorb relatively less energy. Thus, the GFRP/GFRP joint has a larger residual strength. The CFRP/HSS and GFRP/HSS

adhesive joints also show this characteristic. Additionally, the residual life of the adhesive joints with the same adherend is greater than the adhesive joints with dissimilar substrates. It can be concluded that appropriate stiffness matching can contribute to increasing the residual strength within a certain range. The unmatched stiffness may affect the formation of the stress field within the adhesive structure, causing the crack growth rate to be different, which in turn affects the residual properties of joints.

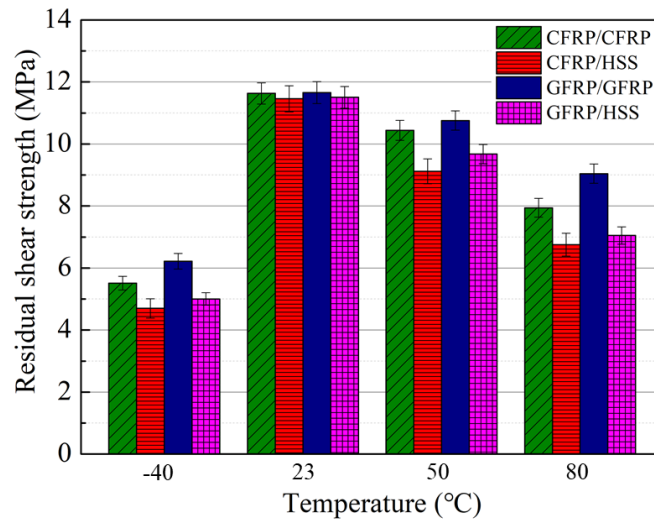


Fig. 17. Residual tensile strength of four types of SLJ ( $E = 1.5$  J).

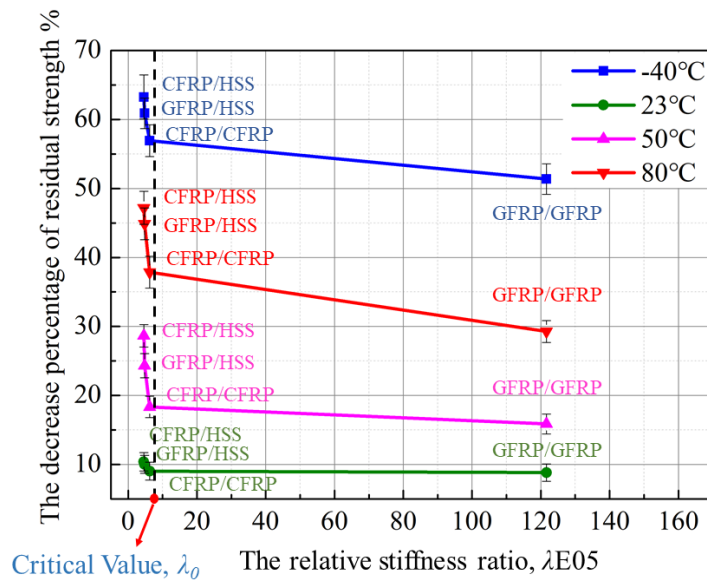


Fig. 18. The percentage decrease of residual tensile strength as a function of the relative stiffness ratio ( $E = 1.5$  J).

A relative stiffness ratio  $\lambda$  is proposed that is expressed as follow:

$$\lambda = \frac{E_i t_i^3 / E_j t_j^3}{(E_i - E_a)(E_j - E_a)} \quad (3)$$

where  $E_a$  is Young's modulus of adhesive material,  $E_j$  and  $t_j$  represent tension modulus and thickness of the stiffer adherend, respectively. The values of the other adherend correspond to  $E_i$  and  $t_i$ , respectively. When the ratio increases, the post-impact carrying capacity of the SLJs could be relatively improved. This ratio provides a clear reference for the design of bonded joints. The post-impact carrying capacity of all types of SLJ — see schematic illustration in Fig. 8 — improved as the stiffness ratio factor increased. Furthermore, the critical value of the stiffness ratio factor  $\lambda_0$  can be obtained. When the stiffness ratio factor of the joint is less than a critical value, the residual mechanical properties are poor; by contrast, when it is greater than the threshold, the joints have better residual performance.

## 6. Conclusions

The low-energy impact at various temperatures and post-impact failure response of four types of SLJ with composites adherends were investigated experimentally. The results indicate that the test temperature, impact kinetic energy and the various combination of the adherends all have a strong impact on the residual tensile properties of composite SLJs. Also, the temperature and impact energy factors have synergistic effects. The key findings are listed below:

- (1) When the specific impact energy (the ratio of impact energy to the mass of the adhesive joint) is less than 117.65 J/kg, there were no obvious dents appearing on the external surface of all the samples.
- (2) The composite adherend may be more sensitive to low temperature than the adhesive under the bending impact loading. The low temperature can easily cause delamination of the composite adherends, especially for joints with mismatched stiffness.
- (3) The critical value of relative stiffness ratio  $\lambda_0$  is proposed as a way of determining the optimal stiffness matching. Only if this stiffness ratio is greater than a threshold

level, will the joints have satisfactory residual strength.

- (4) At -40, 23 and 80 °C, the stiffness and residual strength of the SLJs generally decrease as impact energy increases; while for the 50 °C condition, the residual strength increases as the impact energy increases, mainly due to some sort of crack blunting mechanism near the glass transition temperature transition zone.
- (5) Under 0.5 J impact load conditions, the residual strength of the joint after impact at 80 °C was slightly improved compared to the 50 °C condition.
- (6) More dispersed distribution of residual strength was associated with the joints tested at extreme temperature conditions (-40 or 80 °C), which indicates that the effect of level of impact energy on residual properties increases as the absolute temperature difference increases.

### **Acknowledgement**

The present work was supported by the National Key Research and Development Program of China under Grant No. 2016YFB0101606, and the National Natural Science Foundation of China under Grant Nos. U1664250 and 51575023.

### **References**

- [1] Machado J J M, Gamarra P M R, Marques E A S, et al. Numerical study of the behaviour of composite mixed adhesive joints under impact strength for the automotive industry. *Composite Structures*, 2018, 185:373-380.
- [2] Sayman O, Arikan V, Dogan A, et al. Failure analysis of adhesively bonded composite joints under transverse impact and different temperatures. *Composites Part B: Engineering*, 2013, 54:409-414.
- [3] Qin G, Na J, Tan W, et al. Failure prediction of adhesively bonded CFRP-Aluminum alloy joints using cohesive zone model with consideration of temperature effect. *The Journal of Adhesion*, 2018:1-24.
- [4] Da Silva L F M, Öchsner, Andreas, Adams R D. *Handbook of adhesion technology*. Springer Reference, 2011:1-7.

- [5] De Morais W A, Monteiro S N, d'Almeida J R M. Effect of the laminate thickness on the composite strength to repeated low energy impacts. *Composite structures*, 2005, 70(2): 223-228.
- [6] Tai N H, Yip M C, Lin J L. Effects of low-energy impact on the fatigue behavior of carbon/epoxy composites. *Composites Science and Technology*, 1998, 58(1): 1-8.
- [7] Krollmann J, Schreyer T, Veidt M, et al. Impact and post-impact properties of hybrid-matrix laminates based on carbon fiber-reinforced epoxy and elastomer subjected to low-velocity impacts. *Composite Structures*, 2019, 208: 535-545.
- [8] Liu X, Shao X, Li Q, et al. Experimental study on residual properties of carbon fibre reinforced plastic (CFRP) and aluminum single-lap adhesive joints at different strain rates after transverse pre-impact. *Composites Part A: Applied Science and Manufacturing*, 2019.
- [9] Machado J J M, Nunes P D P, Marques E A S, et al. Adhesive joints using aluminium and CFRP substrates tested at low and high temperatures under quasi-static and impact conditions for the automotive industry. *Composites Part B: Engineering*, 2019, 158: 102-116.
- [10] Artero-Guerrero J A, Pernas-Sánchez J, López-Puente J, et al. Experimental study of the impactor mass effect on the low velocity impact of carbon/epoxy woven laminates. *Composite Structures*, 2015, 133: 774-781.
- [11] Agrawal S, Singh K K, Sarkar P K. Impact damage on fibre-reinforced polymer matrix composite—a review. *Journal of Composite Materials*, 2014, 48(3): 317-332.
- [12] Panettieri E, Fanteria D, Montemurro M, et al. Low-velocity impact tests on carbon/epoxy composite laminates: a benchmark study. *Composites Part B: Engineering*, 2016, 107: 9-21.
- [13] Yang F J, Cantwell W J. Impact damage initiation in composite materials. *Composites Science and Technology*, 2010, 70(2): 336-342.
- [14] Vaidya U K, Gautam A R S, Hosur M, et al. Experimental–numerical studies of transverse impact response of adhesively bonded lap joints in composite structures. *International journal of adhesion and adhesives*, 2006, 26(3): 184-198.

- [15] Kim H, Kayir T, Mousseau S L. Mechanisms of damage formation in transversely impacted glass-epoxy bonded lap joints. *Journal of composite materials*, 2005, 39(22): 2039-2052.
- [16] Sankar H R, Adamvalli M, Kulkarni P P, et al. Dynamic strength of single lap joints with similar and dissimilar adherends. *International Journal of Adhesion and Adhesives*, 2015, 56: 46-52.
- [17] Huang W, Sun L, Li L, et al. Investigations on low-energy impact and post-impact fatigue of adhesively bonded single-lap joints using composites substrates. *The Journal of Adhesion*, 2019: 1-29.
- [18] Ozdemir O, Oztoprak N. An investigation into the effects of fabric reinforcements in the bonding surface on failure response and transverse impact behavior of adhesively bonded dissimilar joints. *Composites Part B: Engineering*, 2017, 126: 72-80.
- [19] Machado J J M, Marques E A S, da Silva L F M. Adhesives and adhesive joints under impact loadings: An overview. *The Journal of Adhesion*, 2018, 94(6): 421-452.
- [20] Grant L D R, Adams R D, da Silva L F M. Effect of the temperature on the strength of adhesively bonded single lap and T joints for the automotive industry. *International journal of adhesion and adhesives*, 2009, 29(5): 535-542.
- [21] Sayman O, Arikan V, Dogan A, et al. Failure analysis of adhesively bonded composite joints under transverse impact and different temperatures. *Composites Part B: Engineering*, 2013, 54: 409-414.
- [22] Sayman O, Soykok I F, Dogan T, et al. Effects of axial impacts at different temperatures on failure response of adhesively bonded woven fabric glass fiber/epoxy composite joints. *Journal of Composite Materials*, 2015, 49(11): 1331-1344.
- [23] Avendaño R, Carbas R J C, Marques E A S, et al. Effect of temperature and strain rate on single lap joints with dissimilar lightweight adherends bonded with an acrylic adhesive. *Composite Structures*, 2016, 152: 34-44.

- [24] Campilho R D S G, Banea M D, Neto J, et al. Modelling of single-lap joints using cohesive zone models: effect of the cohesive parameters on the output of the simulations. *The Journal of Adhesion*, 2012, 88(4-6): 513-533.
- [25] Campilho R, Pinto A M G, Banea M D, et al. Strength improvement of adhesively-bonded joints using a reverse-bent geometry. *Journal of Adhesion Science and Technology*, 2011, 25(18): 2351-2368.
- [26] Campilho R D S G, De Moura M, Pinto A M G, et al. Modelling the tensile fracture behaviour of CFRP scarf repairs. *Composites Part B: Engineering*, 2009, 40(2): 149-157.
- [27] ASTM: D5868-01 Standard test method for lap shear adhesion for fiber reinforced plastic (FRP) bonding.
- [28] Chu Y, Sun L, Zhan B, et al. Static and dynamic behavior of unbalanced bonded joints with adhesion defects in automotive structures. *Composite Structures*, 2019: 111234.
- [29] Kinloch A J, Williams J G. Crack blunting mechanisms in polymers. *Journal of Materials Science*, 1980, 15(4): 987-996.
- [30] Low I M, Mai Y W. Rate and temperature effects on crack blunting mechanisms in pure and modified epoxies. *Journal of materials science*, 1989, 24(5): 1634-1644.
- [31] Yamini S, Young R J. The mechanical properties of epoxy resins. *Journal of materials science*, 1980, 15(7): 1823-1831.
- [32] Hui C Y, Bennison S J, Londono J D. Crack blunting and the strength of soft elastic solids. *Proceedings of the Royal Society of London. Series A: Mathematical, Physical and Engineering Sciences*, 2003, 459(2034): 1489-1516.